

# Structural and luminescent properties of a series of Cd(II) pyridyl benzimidazole complexes that exhibit extended three-dimensional hydrogen bonded networks

Jin-Hua Wang, Gui-Mei Tang, Ting-Xiao Qin, Yong-Tao Wang, Yue-Zhi Cui & Seik Weng Ng

To cite this article: Jin-Hua Wang, Gui-Mei Tang, Ting-Xiao Qin, Yong-Tao Wang, Yue-Zhi Cui & Seik Weng Ng (2017): Structural and luminescent properties of a series of Cd(II) pyridyl benzimidazole complexes that exhibit extended three-dimensional hydrogen bonded networks, Journal of Coordination Chemistry, DOI: [10.1080/00958972.2017.1299143](https://doi.org/10.1080/00958972.2017.1299143)

To link to this article: <http://dx.doi.org/10.1080/00958972.2017.1299143>

 View supplementary material 

 Accepted author version posted online: 28 Feb 2017.  
Published online: 08 Mar 2017.

 Submit your article to this journal 

 Article views: 4

 View related articles 

 View Crossmark data 

## Structural and luminescent properties of a series of Cd(II) pyridyl benzimidazole complexes that exhibit extended three-dimensional hydrogen bonded networks

Jin-Hua Wang<sup>a</sup>, Gui-Mei Tang<sup>a</sup>, Ting-Xiao Qin<sup>a</sup>, Yong-Tao Wang<sup>a</sup>, Yue-Zhi Cui<sup>a</sup> and Seik Weng Ng<sup>b</sup>

<sup>a</sup>Department of Chemical Engineering, Shandong Provincial Key Laboratory of Fine Chemicals, Qilu University of Technology, Jinan, P.R. China; <sup>b</sup>Faculty of Science, Chemistry Department, King Abdulaziz University, Jeddah, Saudi Arabia

### ABSTRACT

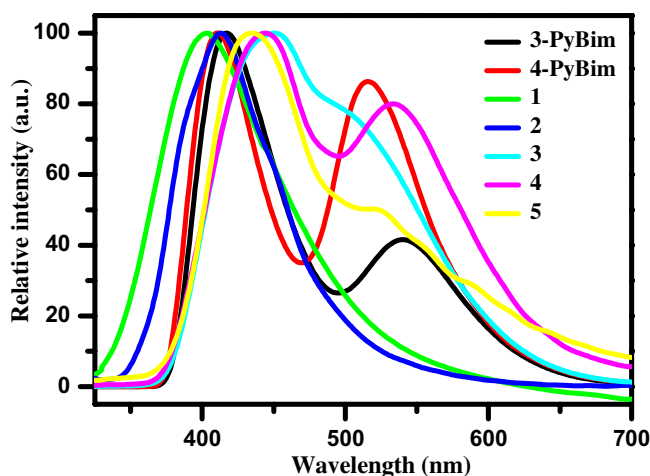
Five new coordination complexes,  $[\text{CdI}_2(\mathbf{3-PyBim})](\text{H}_2\text{O})_3$  (**1**),  $[\text{Cd}(\text{SO}_4)(\mathbf{3-PyBim})(\text{H}_2\text{O})_4]$  (**2**),  $[\text{CdCl}_2(\mathbf{4-PyBim})_2(\text{H}_2\text{O})_2]$  (**3**),  $[\text{CdBr}_2(\mathbf{4-PyBim})_2(\text{H}_2\text{O})_2]$  (**4**) and  $[\text{CdI}_2(\mathbf{4-PyBim})_2(\text{H}_2\text{O})_2]$  (**5**) [**3-PyBim**=2-Pyridin-3-yl-1*H*-benzimidazole, **4-PyBim**=2-Pyridin-4-yl-1*H*-benzimidazole], were obtained under hydrothermal conditions and characterized by single crystal X-ray diffraction, IR, elemental analysis, and powder X-ray diffraction. All of the complexes have mononuclear structures. Among the crystal structures of these complexes, there exist a variety of intermolecular hydrogen bonding interactions and  $\pi \cdots \pi$  interactions, which further extend to a 3-D supramolecular architecture. The solid state photoluminescent properties of **1–5** vary with the electronegativity of the coordination anion. Additionally, the thermogravimetric analyses of these complexes are discussed.

### ARTICLE HISTORY

Received 25 October 2015  
Accepted 13 February 2017

### KEYWORDS

Metal coordination complexes; *N*-heterocyclic ligand; self-assembly; tunable luminescence; cadmium; anions



**CONTACT** Gui-Mei Tang  meiguit@qlu.edu.cn; Yong-Tao Wang  ceswyt@qlu.edu.cn

 Supplemental data for this article can be accessed at <http://dx.doi.org/10.1080/00958972.2017.1299143>.

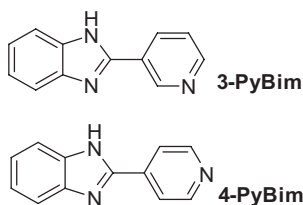
## 1. Introduction

Research has been directed toward coordination complexes that exhibit extended solid state structures [1]. Much of this work has been driven by the ability of such structures to exhibit luminescence [2], drug delivery [3], ferroelectricity [4], non-linear optics [5], gas storage and separation [6], catalysis [7] and magnetism [8]. Several factors need to be taken into account in constructing materials with extended solid state structures, the metal ions [9], the ligands [10], the counter anions [11], the reaction temperature [12], the pH of the reaction [13] and the solvents [14]. The ligands and counter anions play a pivotal role for self-assembly and the structures of final products. To synthesize coordination complexes with the desired extended three-dimensional structures, the choices of ligand, metal ion, and counter ion are critical [15]. Recently, coordination complexes that exhibit extended solid state structures and frameworks have been prepared using *N*-heterocyclic ligands [16]. For example, a series of  $d^{10}$  coordination complexes with pyrazolyl ligands have been reported by Ding *et al.*, and the solid-state luminescent properties revealed that the emission maximum can be tuned from 372 to 486 nm [17]. Although some progress has been made on using coordination complexes as building blocks for extended three-dimensional frameworks, predicted synthesis of such frameworks remains a great challenge.

Coordination complexes of  $d^{10}$  metal ions have interesting luminescence. Their luminescent behavior can be tuned by variation of the organic ligands and the coordinated counter anions [18]. A few metal complexes with excellent fluorescence have been reported [19], and we are interested in incorporating highly luminescent coordination complexes into three-dimensional solid state networks.

We would like to design complexes with interesting luminescence for investigating the relationship between the structures and properties. Therefore, we synthesized two ligands containing *N*-heterocyclic groups, 2-pyridin-3-yl-1*H*-benzoimidazole (**3-PyBim**), and 2-pyridin-4-yl-1*H*-benzoimidazole (**4-PyBim**) (Scheme 1). Both heterocyclic ligands possess the following features: (i) the nitrogen from pyridine can take part in coordinating with metal ions; (ii) two nitrogens from imidazole can act as acceptor and donor of hydrogen bonds, consolidating the thermal stabilities of complexes; (iii) three types of aromatic rings such as pyridine, phenyl, and imidazole can generate  $\pi \cdots \pi$  packing interactions between aromatic rings. Although some coordination complexes with **3-PyBim** [20] and **4-PyBim** [21] have been reported, further development of coordination complexes remains a challenge.

Herein, we report syntheses, solid state structures, and luminescent properties for new supramolecular coordination complexes,  $[\text{CdI}_2(\mathbf{3}\text{-PyBim})_4](\text{H}_2\text{O})_3$  (**1**),  $[\text{Cd}(\text{SO}_4)(\mathbf{3}\text{-PyBim})(\text{H}_2\text{O})_4]$  (**2**),  $[\text{CdCl}_2(\mathbf{4}\text{-PyBim})_2(\text{H}_2\text{O})_2]$  (**3**),  $[\text{CdBr}_2(\mathbf{4}\text{-PyBim})_2(\text{H}_2\text{O})_2]$  (**4**), and  $[\text{CdI}_2(\mathbf{4}\text{-PyBim})_2(\text{H}_2\text{O})_2]$  (**5**), which have been obtained under hydrothermal conditions. Luminescent properties of these complexes can be tuned by the electronegativity of the coordinated anions.



**Scheme 1.** The structures of **3-PyBim** and **4-PyBim**.

## 2. Experimental

### 2.1. Materials and measurements

Reagents and solvents were commercially available and not purified. C, H, and N microanalyses were carried out with a Perkin-Elmer 240 elemental analyzer. The powder X-ray diffraction (PXRD) data were collected on a Bruker D8 diffractometer using Cu-K $\alpha$  radiation. Fluorescence measurements were recorded with an Edinburgh FLS920 fluorescence spectrophotometer. Thermogravimetric analyses (TGA) were carried out on a TA SDT Q600 thermal analyzer under N $_2$  with a heating rate of 10 °C min $^{-1}$  from room temperature to 700 °C. All microwave reactions were carried out on a Galanz G8023CSL-K3 microwave operating at 100 W.

### 2.2. Synthesis of 2-Pyridin-4-yl-1H-benzoimidazole (4-PyBim)

To a mixture solid of isonicotinic acid (1.477 g, 0.012 mol) and 12-phenylene diamine (1.081 mg, 0.010 mol), which were ground and mixed adequately, polyphosphoric acid (10 ml) was added. The reaction mixture was intermittently heated under microwave irradiation with 100-watt power. Subsequently, two blocks of ice were added. The reaction mixture was allowed to cool to room temperature and then poured over water (30 ml). The pH of the reaction mixture was adjusted to 7 by adding 10% NaOH solution. The solid formed was filtered under reduced pressure and dried. Yield (85.9%, 1.675 g). m.p. 224–230 °C. The microanalysis of **4-PyBim** was in accord with those of the compound reported previously [22].

### 2.3. Synthesis of 2-Pyridin-3-yl-1H-benzoimidazole (3-PyBim)

The preparation of **1** was similar to that of **4-PyBim** except that nicotinic acid was used instead of isonicotinic acid. The solid formed was collected and crystallized from pure water to give a needle-like crystal. Yield (76.7%, 1.496 g). m.p. 263–269 °C. The microanalysis of **1** was in agreement with those of the compound reported previously [23].

### 2.4. Synthesis of [CdI $_2$ (3-PyBim) $_4$ ](H $_2$ O) $_3$ (**1**)

A reaction mixture of CdI $_2$  (73.2 mg, 0.2 mmol), **3-PyBim** (19.5 mg, 0.1 mmol), and water (10 ml) was added to a 15 ml Teflon reactor under autogenous pressure at 160 °C for 3 days and then cooled to room temperature at 5 °C h $^{-1}$ . Pale yellow crystals of **1** suitable for diffraction analysis were obtained. (31 mg, Yield: 25.2%). Analysis found (%): C, 48.89; H, 3.50; N, 13.95; requires (%): C, 48.00; H, 3.52; N, 13.99; IR (KBr, cm $^{-1}$ ): 3493 (m), 3169 (w), 3051 (w), 3010 (w), 2993 (w), 2929 (w), 2887 (w), 2794 (w), 2717 (w), 2603 (w), 2189 (w), 1581 (m), 1483 (m), 1433 (s), 1317 (m), 1280 (m), 1226 (m), 1192 (m), 1120 (m), 1047 (m), 966 (m), 923 (w), 817 (m), 744 (s), 700 (m), 638 (m), 408 (w).

### 2.5. Synthesis of [Cd(SO $_4$ )(3-PyBim)(H $_2$ O) $_4$ ]**2**

The preparation of **2** was similar to that of **1** except that Cd(SO $_4$ ) $\cdot$ 8/3H $_2$ O (77.0 mg, 0.1 mmol) was used instead of CdI $_2$  (36.6 mg, 0.1 mmol). Faint pink crystals of **2** were collected. (31 mg,

Yield: 65.2%). Analysis found (%): C, 30.55; H, 3.61; N, 8.80; requires (%): C, 30.29; H, 3.60; N, 8.83; IR (KBr,  $\text{cm}^{-1}$ ): 3206 (br), 3091 (br), 2976 (br), 1589 (w), 1556 (m), 1531 (s), 1489 (s), 1454 (m), 1393 (s), 1317 (w), 1279 (w), 1247 (w), 1229 (w), 1194 (w), 1113 (m), 1107 (m), 1049 (w), 1005 (w), 968 (m), 932 (w), 910 (w), 879 (w), 822 (w), 764 (w), 743 (s), 694 (s), 652 (w), 615 (w), 428 (m), 407 (w).

### 2.6. Synthesis of $[\text{CdCl}_2(4\text{-PyBim})_2(\text{H}_2\text{O})_2]$ (**3**)

A reaction mixture of  $\text{CdCl}_2 \cdot 5/2\text{H}_2\text{O}$  (45.6 mg, 0.2 mmol), **4-PyBim** (19.5 mg, 0.1 mmol), and water (10 ml) was added to a 15 ml Teflon reactor under autogenous pressure at 160 °C for 3 days and then cooled to room temperature at 5 °C  $\text{h}^{-1}$ . Pale yellow crystals of **3** were collected. (23 mg, Yield: 18.9%). Analysis found (%): C, 47.57; H, 3.61; N, 13.73; requires (%): C, 47.27; H, 3.64; N, 13.78; IR (KBr,  $\text{cm}^{-1}$ ): 3510 (m), 3169 (s), 3149 (w), 3118 (w), 3059 (w), 2193 (w), 1938 (w), 1610 (s), 1448 (w), 1381 (w), 1315 (m), 1280 (w), 1230 (w), 1219 (w), 1149 (w), 1107 (w), 1070 (w), 1010 (w), 964 (w), 831 (m), 817 (w), 746 (s), 700 (w), 671 (m), 596 (w), 563 (m), 532 (w), 509 (w), 476 (w), 439 (w).

### 2.7. Synthesis of $[\text{CdBr}_2(4\text{-PyBim})_2(\text{H}_2\text{O})_2]$ (**4**)

The preparation of **4** was similar to that of **3** except that  $\text{CdBr}_2 \cdot 4\text{H}_2\text{O}$  (34.4 mg, 0.1 mmol) was used instead of  $\text{CdCl}_2 \cdot 5/2\text{H}_2\text{O}$  (22.8 mg, 0.1 mmol). Pale yellow crystals of **4** were collected. (31 mg, Yield: 44.3%). Analysis found (%): C, 41.38; H, 3.15; N, 12.05; requires (%): C, 41.26; H, 3.17; N, 12.03; IR (KBr,  $\text{cm}^{-1}$ ): 3520 (m), 3223 (s), 3153 (w), 3116 (w), 3084 (w), 3057 (w), 2993 (w), 2900 (w), 2659 (w), 2084 (w), 2304 (w), 2158 (w), 1639 (m), 1610 (s), 1431 (s), 1313 (m), 1282 (m), 1220 (m), 1147 (m), 1109 (m), 1074 (w), 1012 (m), 972 (m), 823 (m), 752 (s), 698 (m), 644 (m), 561 (m), 511 (m), 437 (m), 414 (m).

### 2.8. Synthesis of $[\text{CdI}_2(4\text{-PyBim})_2(\text{H}_2\text{O})_2]$ (**5**)

The preparation of **5** was similar to that of **3** except that  $\text{CdI}_2$  (36.6 mg, 0.1 mmol) was used instead of  $\text{CdCl}_2 \cdot 5/2\text{H}_2\text{O}$  (22.8 mg, 0.1 mmol). Pale yellow crystals of **5** were collected. (18 mg, Yield: 22.7%). Analysis found (%): C, 36.59; H, 2.82; N, 10.69; requires (%): C, 36.36; H, 2.80; N, 10.60; IR (KBr,  $\text{cm}^{-1}$ ): 3523 (m), 3253 (s), 3151 (w), 3076 (w), 3049 (w), 2897 (w), 2655 (w), 2476 (w), 2324 (w), 2154 (w), 2005 (w), 1629 (m), 1608 (s), 1429 (s), 1311 (m), 1215 (m), 1145 (m), 1008 (m), 970 (m), 823 (m), 750 (s), 696 (m), 613 (m), 559 (m), 511 (m), 408 (m).

### 2.9. Single-crystal structure determination

Single-crystal structure determinations of single crystals of **1–5** were carried out with a Bruker APEX II CCD diffractometer equipped with a graphite crystal monochromator. X-ray intensity data of **1**, **3**, and **5** were measured at 293 K on a Bruker SMART APEX CCD-based diffractometer with graphite-monochromated  $\text{Mo-K}_\alpha$  radiation ( $\lambda = 0.71073 \text{ \AA}$ ), respectively. Data for **4** were collected at 296 K and **2** was done at 100 K. All the measured independent reflections were used in the structural analysis, and semi-empirical

absorption corrections were applied using SADABS [24]. SAINT was used for integration of the diffraction profiles [25]. The structure was solved by direct methods using the SHELXS program of the SHELXTL package and refined with SHELXL [26]. All non-hydrogen atoms were located in successive difference Fourier syntheses. The final refinement was performed by full-matrix least-squares with anisotropic thermal parameters for all the non-hydrogen atoms based on  $F^2$ . The hydrogens were placed in calculated sites and included in the final refinement in the riding model approximation with displacement parameters derived from the parent to which they were bonded. Special computations for the crystal structure discussions were carried out with PLATON for Windows [27]. Crystallographic data and other pertinent information for **1–5** are summarized in Table 1. Selected bond lengths and angles are listed in Table 2. Corresponding hydrogen bonding data are listed in Table 3. The data of weak  $\pi \cdots \pi$  packing interactions are listed in Table 4. Crystallographic data for the structural analysis have been deposited with the Cambridge Crystallographic Data Center; CCDC references numbers are 994345–994350 for **1–5**, respectively. Copies of this information may be obtained free of charge on application to CCDC, 12 Union Road, Cambridge CB2 1EZ, UK (Fax: +44 1223 336 033; E-mail: [deposit@ccdc.cam.ac.uk](mailto:deposit@ccdc.cam.ac.uk) or [www: http://www.ccdc.cam.ac.uk](http://www.ccdc.cam.ac.uk)). Supplementary data associated with this article can be found in the online version.

**Table 1.** Crystal data and structure refinement parameters for **1–5**.

Compound reference	<b>1</b>	<b>2</b>	<b>3</b>	<b>4</b>	<b>5</b>
Chemical formula	C <sub>48</sub> H <sub>42</sub> CdI <sub>2</sub> N <sub>12</sub> O <sub>3</sub>	C <sub>12</sub> H <sub>17</sub> CdN <sub>3</sub> O <sub>8</sub> S	C <sub>24</sub> H <sub>22</sub> CdCl <sub>2</sub> N <sub>6</sub> O <sub>2</sub>	C <sub>24</sub> H <sub>22</sub> Br <sub>2</sub> CdN <sub>6</sub> O <sub>2</sub>	C <sub>24</sub> H <sub>22</sub> CdI <sub>2</sub> N <sub>6</sub> O <sub>2</sub>
Formula mass	1201.14	475.75	609.78	698.70	792.68
Crystal system	Triclinic	Monoclinic	Triclinic	Monoclinic	Monoclinic
<i>a</i> /Å	12.2776(4)	7.8824(5)	7.050(5)	7.06300(10)	7.308(5)
<i>b</i> /Å	12.4178(4)	10.2142(6)	9.236(5)	11.9111(2)	12.250(5)
<i>c</i> /Å	16.5983(6)	19.9949(10)	9.462(5)	14.2997(2)	14.123(5)
$\alpha$ /°	102.386(2)	90.00	76.619(5)	90.00	90.000(5)
$\beta$ /°	107.364(2)	99.768(5)	73.972(5)	96.7570(10)	93.427(5)
$\gamma$ /°	90.110(2)	90.00	87.396(5)	90.00	90.000(5)
Unit cell volume/Å <sup>3</sup>	2353.14(14)	1586.50(16)	576.0(6)	1194.65(3)	1262.1(11)
Temperature/K	293(2)	100(2)	293(2)	296(2)	293(2)
Space group	<i>P</i> –1	<i>P</i> 2 <sub>1</sub> / <i>c</i>	<i>P</i> –1	<i>P</i> 2 <sub>1</sub> / <i>c</i>	<i>P</i> 2 <sub>1</sub> / <i>c</i>
Radiation type	MoK $\alpha$	MoK $\alpha$	MoK $\alpha$	MoK $\alpha$	MoK $\alpha$
Absorption coefficient, $\mu$ mm <sup>–1</sup>	1.832	1.558	1.217	4.295	3.346
No. of reflections measured	32,165	15,730	4855	10,551	11,085
No. of independent reflections	11,542	3679	2770	2976	3125
$R_{\text{int}}$	0.0570	0.0703	0.0266	0.0266	0.0264
Final $R_1$ values ( $I > 2\sigma(I)$ ) <sup>a</sup>	0.0588	0.0529	0.0255	0.0222	0.0217
Final $wR(F^2)$ values ( $I > 2\sigma(I)$ )	0.1458	0.1389	0.0662	0.0548	0.0526
Final $R_1$ values (all data)	0.1085	0.0595	0.0262	0.0267	0.0238
Final $wR(F^2)$ values (all data) <sup>b</sup>	0.1740	0.1418	0.0669	0.0561	0.0536
Goodness of fit on $F^2$	1.025	1.197	1.037	1.056	1.107
CCDC number	994,346	994,347	994,348	994,349	994,350

$$^a R_1 = \frac{\sum |F_o| - |F_c|}{\sum |F_o|}$$

$$^b wR_2 = \frac{[\sum [w(F_o^2 - F_c^2)]^2]}{[\sum w(F_o^2)]^2}^{1/2}$$

**Table 2.** Selected bond lengths (Å) and angles (°) for **1–5**.

<b>1</b>			
Cd1–I1	2.9134(6)	Cd1–I2	2.9076(6)
Cd1–N1	2.422(5)	Cd1–N4	2.448(5)
Cd1–N7	2.455(5)	Cd1–N10	2.434(6)
I1–Cd1–I2	173.81(2)	I1–Cd1–N1	92.70(12)
I1–Cd1–N4	88.04(12)	I1–Cd1–N7	87.13(12)
I1–Cd1–N10	90.95(12)	I2–Cd1–N1	92.06(12)
I2–Cd1–N4	87.24(12)	I2–Cd1–N7	88.66(12)
I2–Cd1–N10	93.36(12)	N1–Cd1–N4	179.08(16)
N1–Cd1–N7	92.95(16)	N1–Cd1–N10	85.76(18)
N4–Cd1–N7	87.63(16)	N4–Cd1–N10	93.69(18)
N7–Cd1–N10	177.64(18)		
<b>2</b>			
Cd1–O1	2.276(3)	Cd1–O1W	2.255(4)
Cd1–O2W	2.343(3)	Cd1–O3W	2.309(4)
Cd1–O4W	2.300(4)	Cd1–N1	2.295(4)
O1–Cd1–O1W	93.00(15)	O1–Cd1–O2W	171.13(14)
O1–Cd1–O3W	90.68(14)	O1–Cd1–O4W	88.22(14)
O1–Cd1–N1	99.49(15)	O1W–Cd1–O2W	79.10(14)
O1W–Cd1–O3W	90.18(14)	O1W–Cd1–O4W	89.79(14)
O1W–Cd1–N1	167.49(16)	O2W–Cd1–O3W	85.38(14)
O2W–Cd1–O4W	95.70(14)	O2W–Cd1–N1	88.49(14)
O3W–Cd1–O4W	178.90(14)	O3W–Cd1–N1	90.29(14)
O4W–Cd1–N1	89.97(14)		
<b>3</b>			
Cd1–Cl1	2.6185(19)	Cd1–O1W	2.364(2)
Cd1–N1	2.332(2)	Cl1–Cd1–N1	90.41(4)
Cl1–Cd1–O1W	93.23(4)	N1–Cd1–N1 <sup>a</sup>	180.00
Cl1–Cd1–Cl1 <sup>a</sup>	180.00	O1W–Cd1–N1	87.74(6)
Cl1–Cd1–N1 <sup>a</sup>	89.59(4)	O1W–Cd1–O1W <sup>a</sup>	180.00
O1W–Cd1–Cl1 <sup>a</sup>	86.77(4)		
O1W–Cd1–N1 <sup>a</sup>	92.26(6)		
<b>4</b>			
Cd1–Br1	2.7213(2)	Cd1–O1W	2.3656(15)
Cd1–N1	2.3434(16)	Br1–Cd1–N1	89.39(4)
Br1–Cd1–O1W	89.23(4)	N1–Cd1–N1 <sup>b</sup>	180.00
Br1–Cd1–Br1 <sup>b</sup>	180.00	O1W–Cd1–N1	89.18(5)
Br1–Cd1–N1 <sup>b</sup>	90.61(4)	O1W–Cd1–O1W <sup>b</sup>	180.00
O1W–Cd1–Br1 <sup>b</sup>	90.77(4)		
O1W–Cd1–N1 <sup>b</sup>	90.82(5)		
<b>5</b>			
I1–Cd1	2.885(2)	Cd1–N1	2.377(3)
Cd1–O1W	2.355(3)	O1W–Cd1–N1	89.12(7)
I1–Cd1–O1W	90.07(5)	N1–Cd1–N1 <sup>c</sup>	180.00
I1–Cd1–N1	89.55(5)	O1W–Cd1–O1W <sup>c</sup>	180.00
I1–Cd1–I1 <sup>c</sup>	180.00	O1W–Cd1–N1 <sup>c</sup>	90.88(7)
I1–Cd1–O1W <sup>c</sup>	89.93(5)		
I1–Cd1–N1 <sup>c</sup>	90.45(5)		

Symmetry codes: <sup>a</sup>1 – x, 1 – y, 1 – z. <sup>b</sup>–x, 1 – y, 1 – z. <sup>c</sup>–x, 1 – y, 1 – z.

### 3. Results and discussion

#### 3.1. Description of the crystal structures

##### 3.1.1. Structure description of $[CdI_2(3\text{-PyBim})](H_2O)_3$ (**1**)

The results of X-ray crystallographic analysis reveal that **1** is mononuclear, crystallizing in the triclinic *P*-1 space group. One Cd, four **3-PyBim** ligands, two iodides, and three water molecules exist in the asymmetric unit. As illustrated in Figure 1(a), Cd is six-coordinate with a distorted octahedral coordination environment surrounded by four nitrogens from four **3-PyBim** ligands and two iodides. The bond distances of Cd–N in **1** vary from 2.422(5) to

**Table 3.** Hydrogen bond geometries in the crystal structure of **1–5**.

Complex	D–H···A <sup>a</sup>	H···A (Å)	D···A (Å)	D–H···A (°)
1	O1W–H1···N2	2.00	2.755(7)	148
	O1W–H2···N6 <sup>a</sup>	1.93	2.728(7)	155
	N2–H2···O1W	1.91	2.755(7)	162
	O2W–H3···N11	2.01	2.764(7)	148
	O2W–H4···N8 <sup>b</sup>	1.90	2.713(7)	160
	N6–H6···O1W <sup>a</sup>	1.75	2.728(7)	151
	N9–H9···N12 <sup>c</sup>	2.02	2.855(7)	167
	N11–H11···O2W	1.94	2.764(7)	149
	C1–H1A···O1W	2.45	3.362(8)	166
	C3–H37···O2W	2.43	3.351(8)	168
2	N3–H3···O4 <sup>d</sup>	1.99	2.861(6)	168
	O1W–H11···O2 <sup>e</sup>	2.30	3.038(6)	147
	O1W–H12···N2 <sup>e</sup>	1.85	2.691(5)	179
	O2W–H21···O2 <sup>e</sup>	1.96	2.759(6)	158
	O2W–H22···O3 <sup>f</sup>	1.93	2.759(5)	172
	O3W–H31···O3	2.03	2.799(6)	153
	O3W–H32···O1 <sup>e</sup>	1.97	2.772(6)	161
	O4W–H41···O4 <sup>g</sup>	2.03	2.860(6)	168
	O4W–H42···O2 <sup>f</sup>	1.88	2.722(6)	177
	C4–H4···O3W <sup>h</sup>	2.41	3.263(5)	150
3	C5–H5···O2W	2.48	3.140(6)	127
	C10–H10···O3 <sup>f</sup>	2.51	3.262(7)	136
	O1W–H1···N3 <sup>i</sup>	1.95	2.798(3)	172
	N2–H2···Cl1 <sup>j</sup>	2.31	3.170(3)	164
4	O1W–H3···Cl1 <sup>k</sup>	2.59	3.438(3)	166
	O1W–H1WA···N3 <sup>l</sup>	1.97	2.791(3)	172
5	O1W–H1WB···Br1 <sup>m</sup>	2.76	3.4869(14)	150
	N2–H2A···Br1 <sup>l</sup>	2.5	3.3768(18)	161
	O1W–H1WA···N3 <sup>n</sup>	1.96	2.807(3)	173
5	O1W–H1WB···I1 <sup>o</sup>	2.91	3.666(3)	150
	N2–H2A···I1 <sup>n</sup>	2.73	3.593(3)	160

Symmetry codes: <sup>a</sup>1 – x, –y, 1 – z. <sup>b</sup>1 – x, 1 – y, 1 – z. <sup>c</sup>–x, 1 – y, 1 – z. <sup>d</sup>x, 1/2 – y, 1/2 + z. <sup>e</sup>1 – x, 1/2 + y, 1/2 – z. <sup>f</sup>–1 + x, y, z. <sup>g</sup>1 – x, –1/2 + y, 1/2 – z. <sup>h</sup>1 – x, 1 – y, 1 – z. <sup>i</sup>2 – x, –y, 1 – z. <sup>j</sup>1 – x, –y, 1 – z. <sup>k</sup>x, y, –1 + z. <sup>l</sup>–1 + x, y, z. <sup>m</sup>–x, 1/2 + y, 3/2 – z. <sup>n</sup>–1 – x, 1 – y, 1 – z. <sup>o</sup>–x, 1/2 + y, 3/2 – z. <sup>p</sup>–1 – x, 1 – y, 1 – z.

2.455(5) Å; the bond lengths of Cd–I are 2.9076(6) to 2.9134(6) Å, in agreement with those published previously [28].

As illustrated in Figure 1(b), one O–H···N intermolecular hydrogen bond was formed between the free water molecules and nitrogens from the imidazole groups (O1W–H1···N2, O1W–H2···N6<sup>a</sup>, O2W–H3···N11 and O2W–H4···N8<sup>b</sup> distances of 2.755(7), 2.728(7), 2.764(7) and 2.713(7) Å, respectively, <sup>a</sup>1 – x, –y, 1 – z, <sup>b</sup>1 – x, 1 – y, 1 – z), through which a 1-D supra-molecular chain is generated.

There also exist three kinds of intermolecular hydrogen bonds in **1**: (i) N–H···O intermolecular hydrogen bonds form between nitrogens of imidazole and free water molecules (N2–H2···O1W, N6–H6···O1W<sup>a</sup> and N11–H11···O2W distances of 2.755(7), 2.728(7) and 2.764(7) Å, respectively, <sup>a</sup>1 – x, –y, 1 – z); (ii) The N–H···N intermolecular hydrogen bond comes from nitrogens of imidazoles and other nitrogens of imidazoles (N9–H9···N12<sup>c</sup> distance of 2.855(7) Å, <sup>c</sup>–x, 1 – y, 1 – z); (iii) Intermolecular hydrogen bonds originate from carbons of pyridine groups and free water molecules (C1–H1A···O1W and C3–H37···O2W distances of 3.362(8) and 3.351(8) Å, respectively). The inter-hydrogen bonds alternate and

**Table 4.** Weak  $\pi \cdots \pi$  packing interactions for **1–5**.

Complexes		Distance (Å)	Average distance (Å)
<b>1</b> <sup>i</sup>	Cg(12)⋯Cg(5) <sup>a</sup>	3.797(4)	3.797
	Cg(5)⋯Cg(12) <sup>a</sup>	3.797(4)	
<b>2</b> <sup>ii</sup>	Cg(1)⋯Cg(1) <sup>c</sup>	3.359(3)	3.552
	Cg(1)⋯Cg(2) <sup>b</sup>	3.422(3)	
	Cg(1)⋯Cg(3) <sup>c</sup>	3.544(3)	
	Cg(2)⋯Cg(1) <sup>b</sup>	3.422(3)	
	Cg(2)⋯Cg(3) <sup>b</sup>	3.785(3)	
	Cg(3)⋯Cg(1) <sup>c</sup>	3.544(3)	
	Cg(3)⋯Cg(2) <sup>b</sup>	3.785(3)	
<b>3</b> <sup>iii</sup>	Cg(1)⋯Cg(1) <sup>d</sup>	3.566(3)	3.610
	Cg(2)⋯Cg(3) <sup>e</sup>	3.649(3)	
	Cg(2)⋯Cg(3) <sup>d</sup>	3.594(3)	
	Cg(3)⋯Cg(2) <sup>d</sup>	3.649(3)	
	Cg(3)⋯Cg(2) <sup>d</sup>	3.594(3)	
<b>4</b> <sup>iv</sup>	Cg(1)⋯Cg(1) <sup>f</sup>	3.5679(12)	3.680
	Cg(2)⋯Cg(3) <sup>e</sup>	3.6813(12)	
	Cg(2)⋯Cg(3) <sup>f</sup>	3.7347(12)	
	Cg(3)⋯Cg(2) <sup>e</sup>	3.6813(12)	
	Cg(3)⋯Cg(2) <sup>f</sup>	3.7347(12)	
<b>5</b> <sup>v</sup>	Cg(1)⋯Cg(1) <sup>g</sup>	3.715(3)	3.760
	Cg(2)⋯Cg(3) <sup>h</sup>	3.783(3)	
	Cg(3)⋯Cg(2) <sup>g</sup>	3.783(3)	

Symmetry codes: <sup>a</sup> $-x, 1-y, 1-z$ . <sup>b</sup> $1-x, -y, 1-z$ . <sup>c</sup> $2-x, -y, 1-z$ . <sup>d</sup> $1-x, -y, -z$ . <sup>e</sup> $2-x, -y, -z$ . <sup>f</sup> $-x, 1-y, 2-z$ . <sup>g</sup> $1-x, 1-y, 2-z$ . <sup>h</sup> $-x, 1-y, 2-z$ . <sup>i</sup> $1-x, 1-y, 2-z$ . <sup>ii</sup>The rings Cg(5) and Cg(2) are expressed by N(1)–C(1)–C(2)–C(3)–(4)–C(5) and C(43)–C(44)–C(45)–C(46)–C(47)–C(48), respectively. <sup>iii</sup>The rings Cg(1), Cg(2), and Cg(3) consisted of N(2)–C(6)–N(3)–C(12)–C(7), N(1)–C(1)–C(2)–C(3)–(4)–C(5), and C(7)–C(8)–C(9)–C(10)–C(11)–C(12), respectively. <sup>iv</sup>The rings Cg(1), Cg(2), and Cg(3) denote N(2)–C(6)–N(3)–C(12)–C(7), N(1)–C(1)–C(2)–C(3)–(4)–C(5), and C(7)–C(8)–C(9)–C(10)–C(11)–C(12), respectively. <sup>v</sup>The rings Cg(1), Cg(2), and Cg(3) contain N(2)–C(6)–N(3)–C(12)–C(7), N(1)–C(1)–C(2)–C(3)–(4)–C(5), and C(7)–C(8)–C(9)–C(10)–C(11)–C(12), respectively. <sup>v</sup>The rings Cg(1), Cg(2), and Cg(3) consisted of N(2)–C(6)–N(3)–C(12)–C(7), N(1)–C(1)–C(2)–C(3)–(4)–C(5), and C(7)–C(8)–C(9)–C(10)–C(11)–C(12), respectively.

consolidate the stacked arrangement leading to a two-dimensional layer along the *ab* plane (Figure 1(c)).

Weak C–H⋯ $\pi$  interactions occur between carbons from phenyl groups and other phenyls (C9–H9A⋯ $\pi_{(C19-C24)}$ , C21–H21A⋯ $\pi_{(C43-C48)}$ , C34–H34A⋯ $\pi_{(N7-C12)}$  and C46–H46A⋯ $\pi_{(C31-C36)}$  with distances of 3.621(7), 3.576(8), 3.845(8), and 3.611(8) Å, respectively). Consequently, a 3-D supramolecular architecture is constructed through these hydrogen bonding and weak packing interactions (Figure 1(d)).

### 3.1.2. Structure description of [Cd(SO<sub>4</sub>)(3-PyBim)(H<sub>2</sub>O)<sub>4</sub>] (**2**)

When changing from CdI<sub>2</sub> to Cd(SO<sub>4</sub>), **2** possessing a mononuclear structure was obtained. Complex **2** crystallizes in the monoclinic space group *P2<sub>1</sub>/c*. As illustrated in Figure 2(a), the asymmetric unit of **2** is composed of one Cd(II), one **3-PyBim** ligand, one sulfate, and four coordinated waters. The coordination geometry around Cd(II) is six coordinate with a distorted octahedral geometry by one nitrogen from a pyridine ring and five oxygens from one sulfate and four different water molecules. The Cd–O bond distances in **2** are 2.255(4)–2.343(3) Å; the Cd–N bond length is 2.295(4) Å, all in agreement with those published previously [28].

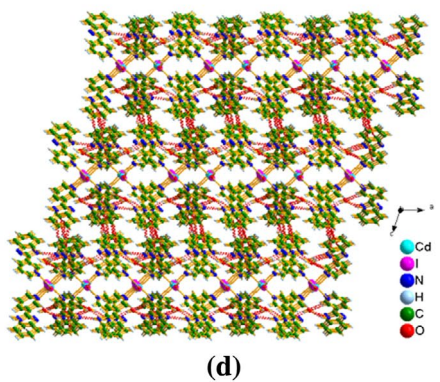
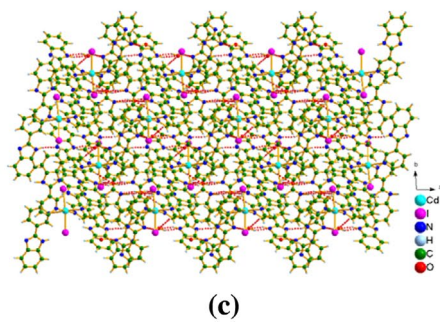
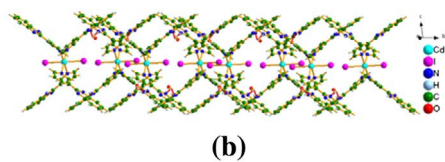
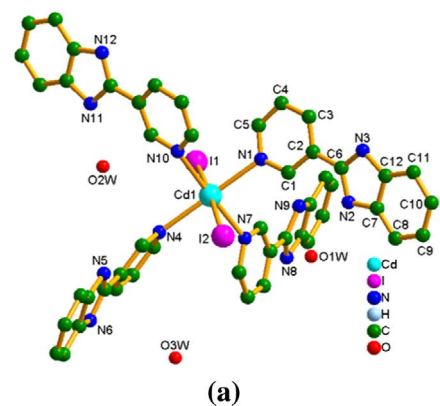


**Figure 1.** (a) A perspective view of the coordination geometry of Cd in 1. (b) A one-dimensional chain through hydrogen bonds along the *b* axis. (c) A two-dimensional layer along the *ab* plane in 1. (d) The packing diagram of 1.

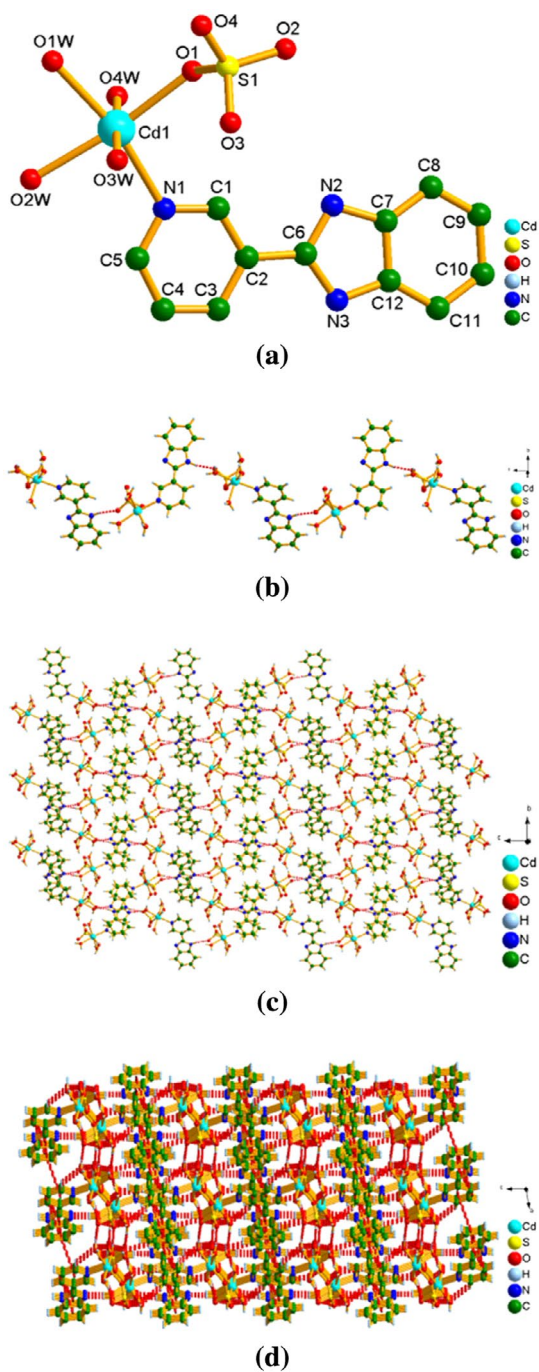


**Figure 2.** (a) A perspective view of the coordination geometry of Cd in **2**. (b) A one-dimensional chain through hydrogen bonds along the *c* axis. (c) A two-dimensional layer along the *bc* plane in **2**. (d) The topology structure of **2**.

The supramolecular structure depends on many kinds of hydrogen bonding interactions. As illustrated in Figure 2(b), one hydrogen bond is generated through the nitrogens from imidazole and the oxygens from sulfate ( $\text{N3-H3}\cdots\text{O4}^{\text{d}}$  distance of 2.861(6) Å,  $^{\text{d}}x, 1/2 - y, 1/2 + z$ ), through which a 1-D supramolecular chain is generated.

Additionally, hydrogen bonding occurs between oxygens from sulfates and nitrogens from imidazole ( $\text{O1W-H12}\cdots\text{N2}^{\text{e}}$  distance of 2.691(5) Å,  $^{\text{e}}1 - x, 1/2 + y, 1/2 - z$ ). Thus, a 2-D supramolecular layer is further generated through these hydrogen bonding interactions (Figure 2(c)).

Apart from these interactions, there also exist other weak hydrogen bonding interactions and weak packing interactions, which consolidate the stacked arrangement leading to a 3-D supramolecular architecture. There exist three kinds of weak hydrogen bonding interactions: (i) the coordinated water molecules and coordinated sulfate ( $\text{O1W-H11}\cdots\text{O2}^{\text{e}}$ ,  $\text{O2W-H21}\cdots\text{O2}^{\text{e}}$ ,  $\text{O2W-H22}\cdots\text{O3}^{\text{f}}$ ,  $\text{O3W-H31}\cdots\text{O3}$ ,  $\text{O3W-H32}\cdots\text{O1}^{\text{e}}$ ,  $\text{O4W-H41}\cdots\text{O4}^{\text{g}}$  and  $\text{O4W-H42}\cdots\text{O2}^{\text{f}}$  distances of 2.759(6), 2.759(5), 2.799(6), 2.772(6), 2.860(6), 2.722(6), and 3.038(6) Å, respectively,  $^{\text{e}}1 - x, 1/2 + y, 1/2 - z$ ,  $^{\text{f}}-1 + x, y, z$  and  $^{\text{g}}1 - x, -1/2 + y, 1/2 - z$ ); (ii) carbons of pyridine rings and coordinated water ( $\text{C4-H4}\cdots\text{O3W}^{\text{h}}$  and  $\text{C5-H5}\cdots\text{O2W}$  distances of 3.263(5) and 3.140(6) Å, respectively,  $^{\text{h}}1 - x, 1 - y, 1 - z$ ); (iii) carbons of phenyl rings and oxygens of coordinated sulfate ( $\text{C10-H10}\cdots\text{O3}^{\text{i}}$  distance of 3.262(7) Å,  $^{\text{i}}2 - x, -y, 1 - z$ ). There also exist a series of weak  $\pi\cdots\pi$  packing interactions ( $\text{Cg}(1)\cdots\text{Cg}(1)^{\text{c}}$ ,  $\text{Cg}(1)\cdots\text{Cg}(2)^{\text{b}}$ ,  $\text{Cg}(1)\cdots\text{Cg}(3)^{\text{c}}$ ,  $\text{Cg}(2)\cdots\text{Cg}(1)^{\text{b}}$ ,  $\text{Cg}(2)\cdots\text{Cg}(3)^{\text{b}}$ ,  $\text{Cg}(3)\cdots\text{Cg}(1)^{\text{c}}$ , and  $\text{Cg}(3)\cdots\text{Cg}(2)^{\text{b}}$  distances of 3.359(3), 3.422(3), 3.544(3), 3.422(3), 3.785(3), 3.544(3), and 3.785(3) Å, respectively,  $^{\text{b}}1 - x, -y, 1 - z$  and  $^{\text{c}}2 - x, -y, 1 - z$ . Cg(1), Cg(2), and Cg(3) are indicated as imidazole ring, pyridine ring, and benzene ring, respectively) (Figure 2(d), Table 3). Consequently, through these hydrogen bonding and weak packing interactions, a 3-D supramolecular architecture is constructed (Figure 2(d)).

### 3.1.3. Structure description of $[\text{CdCl}_2(4\text{-PyBim})_2(\text{H}_2\text{O})_2] \mathbf{3}$

Single-crystal X-ray analysis reveals that **3** is a mononuclear structure which crystallizes in the form of the centrosymmetric space group  $P-1$ . As shown in Figure 3(a), the asymmetric unit contains one Cd(II), one **4-PyBim** ligand, one coordinated water, and one chloride. Cd1 is six-coordinate with two nitrogens from two **4-PyBim** ligands, two oxygens from two water molecules, and two chlorides in a slightly distorted octahedral configuration. The bond distances of Cd-Cl, Cd-O, and Cd-N in **3** are 2.6185(19), 2.364(2), and 2.332(2) Å, respectively, in agreement with those published previously [28].

The supramolecular structure mainly depends on many hydrogen bonding interactions originating from coordinated waters as donor/acceptors, nitrogens of the imidazole rings and coordinated chlorides. There are three kinds of intermolecular hydrogen bonds in **3**: (i) intermolecular hydrogen bonding between coordinated water and coordinated chlorides ( $\text{O1W-H3}\cdots\text{Cl1}^{\text{k}}$ , 3.438(3) Å,  $^{\text{k}}-1 + x, y, z$ ), generating a 1-D supramolecular chain along the  $a$  axis in **3** (Figure 3(b)); (ii) intermolecular hydrogen bonding between coordinated water and nitrogens from imidazole ( $\text{O1W-H1}\cdots\text{N3}^{\text{l}}$ , 2.798(3) Å,  $^{\text{l}}1 - x, -y, 1 - z$ ). Thus, a two-dimensional supramolecular layer is formed by this kind of hydrogen bonding on the basis of 1-D supramolecular chains in **3** (Figure 3(c)); (iii) The  $\text{N2-H2}\cdots\text{Cl1}^{\text{j}}$  (3.170(3) Å,  $^{\text{j}}x, y, -1 + z$ ) intermolecular hydrogen bonding comes from nitrogens of the imidazole rings and coordinated chlorides. The supramolecular interactions are propitious to form a 3-D supramolecular architecture via weak hydrogen bonding interactions mentioned above (Figure 3(d)).

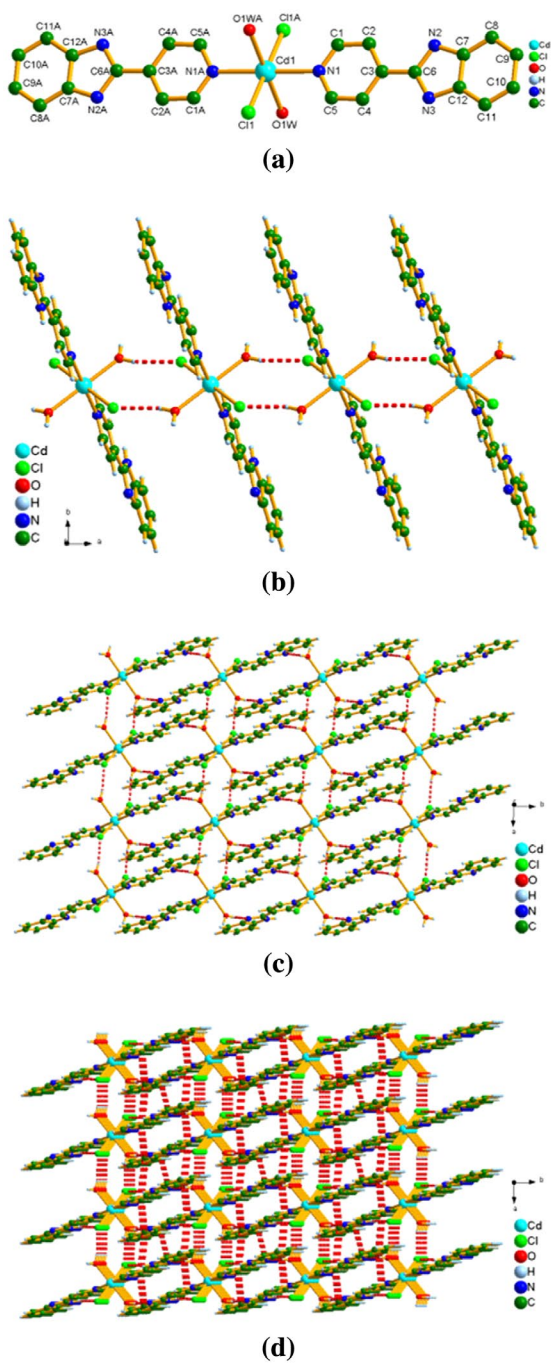


**Figure 3.** (a) A perspective view of the coordination geometry of Cd in **3**. (b) A one-dimensional chain through hydrogen bonds along the *a* axis. (c) A two-dimensional layer along the *ab* plane in **3**. (d) The packing diagram of **3**.

There also exist two kinds of weak  $\pi \cdots \pi$  packing interactions between the aromatic rings. One occurs between pyridine groups and benzene (3.594(3) and 3.649(3) Å) and another between two imidazole groups (3.5679(12) Å). These weak packing interactions consolidate a three-dimensional supramolecular framework (Figure 3(d)).

### 3.1.4. Structure description of $[\text{CdBr}_2(\text{4-PyBim})_2(\text{H}_2\text{O})_2]$ (**4**)

When  $\text{CdCl}_2$  was changed to  $\text{CdBr}_2$ , **4** crystallizes in the monoclinic space group  $P2_1/c$ . Complex **4** is also mononuclear. As illustrated in Figure 4(a), the asymmetric unit of **5** has one Cd(II), one **4-PyBim** ligand, one bromide, and one coordinated water. The coordination geometry around Cd(II) is six coordinate with a distorted octahedral geometry, surrounded by two nitrogens from two different **4-PyBim** ligands, two oxygens from two coordinated waters and two bromides. The Cd-Br, Cd-O, and Cd-N bond distances in **4** are 2.7213(2), 2.3656(15), and 2.3434(16) Å, respectively, in agreement with those published previously [28].

As illustrated in Figure 4(b), a hydrogen bond is generated through the coordinated water and bromides ( $\text{O1W-H1WB} \cdots \text{Br1}^i$  distance of 3.4869(14) Å,  $^i -1 - x, 1 - y, 1 - z$ ), through which a 1-D supramolecular chain is generated along the  $a$  axis.

Apart from the  $\text{O-H} \cdots \text{Br}$  intermolecular hydrogen bond, there also exist two weak  $\pi \cdots \pi$  packing interactions between aromatic rings. One originates from the pyridine and benzene (3.6813(12) and 3.7347(12) Å) and another from two imidazole groups (3.5679(12) Å). These weak  $\pi \cdots \pi$  packing interactions and the  $\text{O-H} \cdots \text{Br}$  hydrogen bond lead to a 2-D supramolecular layer (Figure 4(c)).

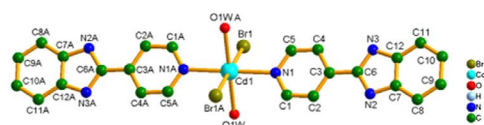
There exist two other kinds of weak hydrogen bonding interactions: (i)  $\text{O1W-H1WA} \cdots \text{N3}^i$  (2.791(3) Å,  $^i -x, 1/2 + y, 3/2 - z$ ) intermolecular hydrogen bonding between coordinated water and nitrogen from imidazole; (ii)  $\text{N2-H2A} \cdots \text{Br1}^i$  (3.3768(18) Å,  $^i -x, 1/2 + y, 3/2 - z$ ) intermolecular hydrogen bonding between the coordinate bromides and nitrogens from imidazole. These hydrogen-bonding patterns A–D (Acceptor–Donor) construct a 3-D supramolecular architecture in **4** (Figure 4(d)).

### 3.1.5. Structure description of $[\text{CdI}_2(\text{4-PyBim})_2(\text{H}_2\text{O})_2]$ (**5**)

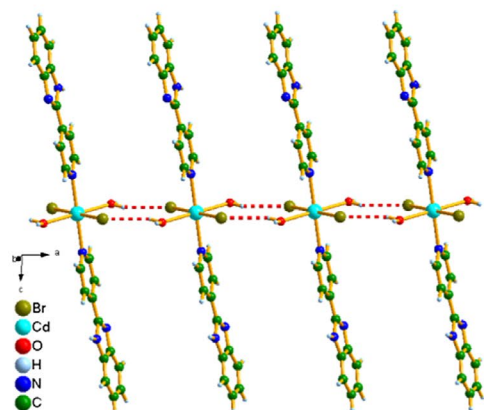
X-ray crystallographic analysis showed that **5** is also mononuclear, crystallizing in the monoclinic space group  $P2_1/c$ . As illustrated in Figure 5(a), one Cd(II), one **4-PyBim** ligand, one iodide, and one coordinated water exist in the asymmetric unit. The coordination geometry around Cd(II) is six coordinate with a distorted octahedral geometry from two nitrogens of two different **4-PyBim** ligands, two oxygens from two coordinated water molecules and two iodides (Figure 5(a)). The bond distances of Cd-O and Cd-N are 2.355(3) and 2.377(3) Å, respectively, similar to those found in complexes reported previously [28].

Similar to **4**, a hydrogen bond is generated through the coordinated water molecule and iodide ( $\text{O1W-H1WB} \cdots \text{I1}^n$  3.666(3) Å,  $^n -1 - x, 1 - y, 1 - z$ ), through which a 1-D supramolecular chain is generated along the crystallographic  $a$  axis (Figure 5(b)).

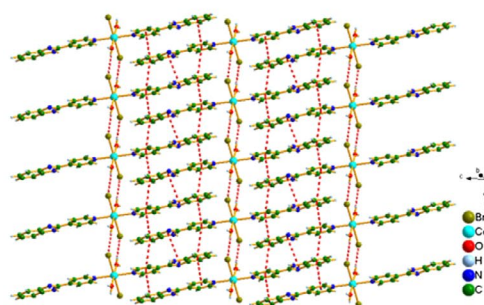
Two kinds of weak  $\pi \cdots \pi$  packing interactions exist between the aromatic rings, one from pyridine and benzene (3.783(3) Å) and another from two imidazole groups (3.715(3) Å). As a result, a 2-D supramolecular layer based on these supramolecular interactions is constructed (Figure 5(c)).



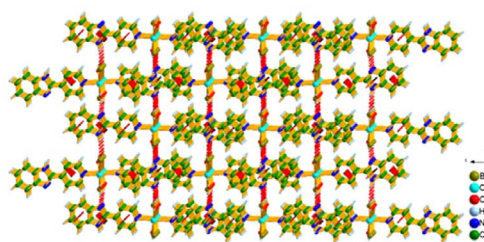
(a)



(b)



(c)



(d)

**Figure 4.** (a) A perspective view of the coordination geometry of Cd in **4**. (b) A one-dimensional chain through hydrogen bonds along the *a* axis. (c) A two-dimensional layer along the *ac* plane in **4**. (d) The packing diagram of **4**.

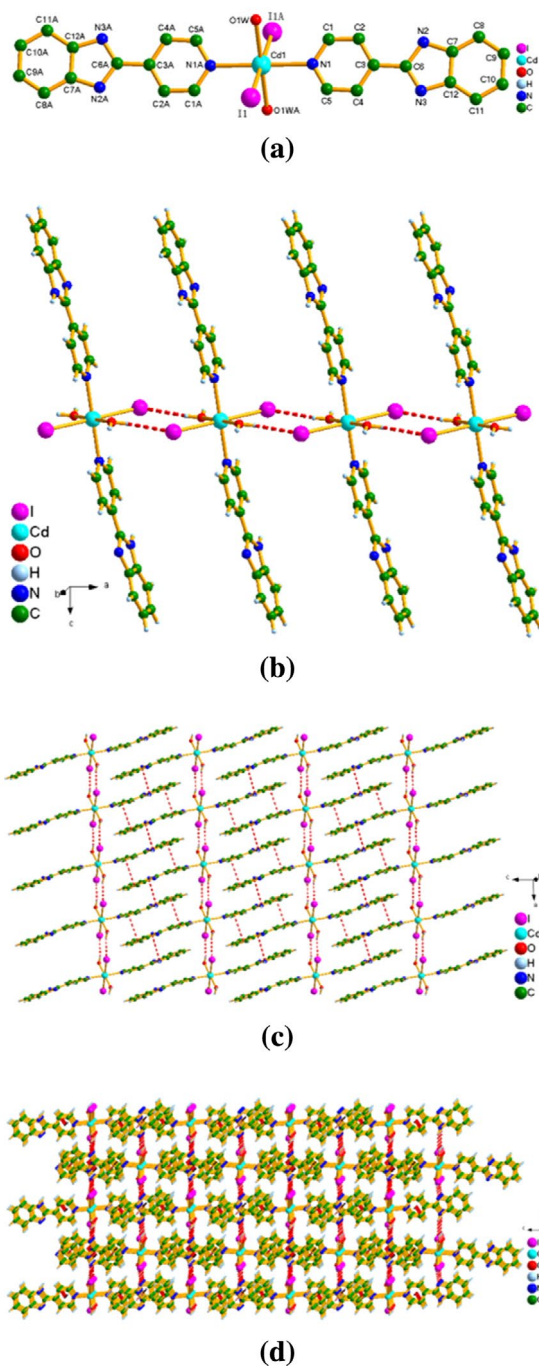


**Figure 5.** (a) A perspective view of the coordination geometry of Cd in **5**. (b) A one-dimensional chain through hydrogen bonds along the *a* axis. (c) A two-dimensional layer along the *ac* plane in **5**. (d) The packing diagram of **5**.

Two other hydrogen bonds are observed: (i) O1W–H1WA $\cdots$ N3<sup>n</sup> (2.807(3) Å, <sup>n</sup>–*x*, 1/2 + *y*, 3/2 – *z*) intermolecular hydrogen bond forms between the coordinated water and nitrogen from imidazole; (ii) N2–H2A $\cdots$ I1<sup>n</sup> (3.593(3) Å, <sup>n</sup>–*x*, 1/2 + *y*, 3/2 – *z*) intermolecular hydrogen bond between nitrogen from the imidazole rings and iodide. Consequently, a 3-D supramolecular architecture is interestingly founded via the three types of hydrogen-bonded patterns A–D mentioned above and other weak packing interactions in **5** (Figure 5(d)).

### 3.2. Powder X-ray diffraction (XRD) patterns and thermogravimetric analyses (TGA)

To confirm the phase purity of the five complexes, the XRD patterns were recorded. Most of the peak positions of the simulated and experimental patterns are in agreement with each other (Figures S1–S5). The present results show that products are a pure phase.

To estimate the stability of the coordination architectures of **1–5**, TGA were carried out. The experiments were performed on powder samples of **1–5** under nitrogen with a heating rate of 10 °C min<sup>–1</sup> (Figures S6–S10 in the Supporting Information). Complex **1** lost its coordinated water from room temperature to 136 °C (obsd 5.9%, calcd 4.50%). The anhydrous compound begins to decompose at 247 °C, leading to formation of CdO as the residue (obsd 9.41%, calcd 10.69%). For **2**, the first weight loss corresponding to release of coordinated water is observed before 177 °C (obsd 13.85%, calcd 15.13%), and the organic components were lost from 290 °C. The final residue of 22.98% (calcd 26.99%) is observed, which indicates that formation of CdO is generated. The TGA curve of **3** shows that the first weight loss occurs from 70–241 °C (obsd 4.56%, calcd 5.90%), indicating that coordinated water molecules are lost. Decomposition of the anhydrous compound occurs from 296 to 762 °C. The final weight of 18.00% (calcd 21.06%) is observed, corresponding to formation of cadmium oxide. For **4**, weight loss from 56 to 233 °C corresponds to loss of coordinated water (obsd 6.3%, calcd 5.3%); removal of the organic components occurs from 260 to 520 °C. The remaining weight corresponds to CdO (obsd 12.78%, calcd 18.38%). Complex **5** lost its coordinated water molecules from 68 to 172 °C (obsd 4.32%, calcd 4.54%). The anhydrous compound begins to decompose at 225 °C. The weight of the final compound is 11.57% (calcd 16.20%), which can tentatively be assigned to CdO.

### 3.3. Photoluminescent properties

In view of the excellent luminescent properties of d<sup>10</sup> metal coordination complexes [29], the solid state luminescence properties of **1–5** were studied at room temperature. The emission spectra have broad peaks with maxima at 404, 413, 451, 444, and 435 nm ( $\lambda_{\text{ex}} = 280$  nm) for **1–5**, respectively. To compare the emission bands for complexes, we have also investigated the luminescence properties of the two free ligands in the solid state at room temperature. As indicated in Figure 6(a) and (b), the emission maxima were observed at 417 and 540 nm for free **3-PyBim**, 411 and 516 nm for **4-PyBim**, and are attributed to the  $\pi^* \rightarrow \pi$  transition. Compared with the emission peaks of free **3-PyBim**, the emission maxima for **1** and **2** are blue-shifted about 4 and 13 nm, respectively. The present results could be assigned to intra-ligand  $\pi^* \rightarrow \pi$  transition. In comparison with the emission peaks of free **4-PyBim**, those of **3–5** are red-shifted about 40, 33, and 24 nm, respectively, which may be ascribed to the intra-ligand  $\pi^* \rightarrow \pi$  transition. Luminescence intensities of all the complexes are stronger

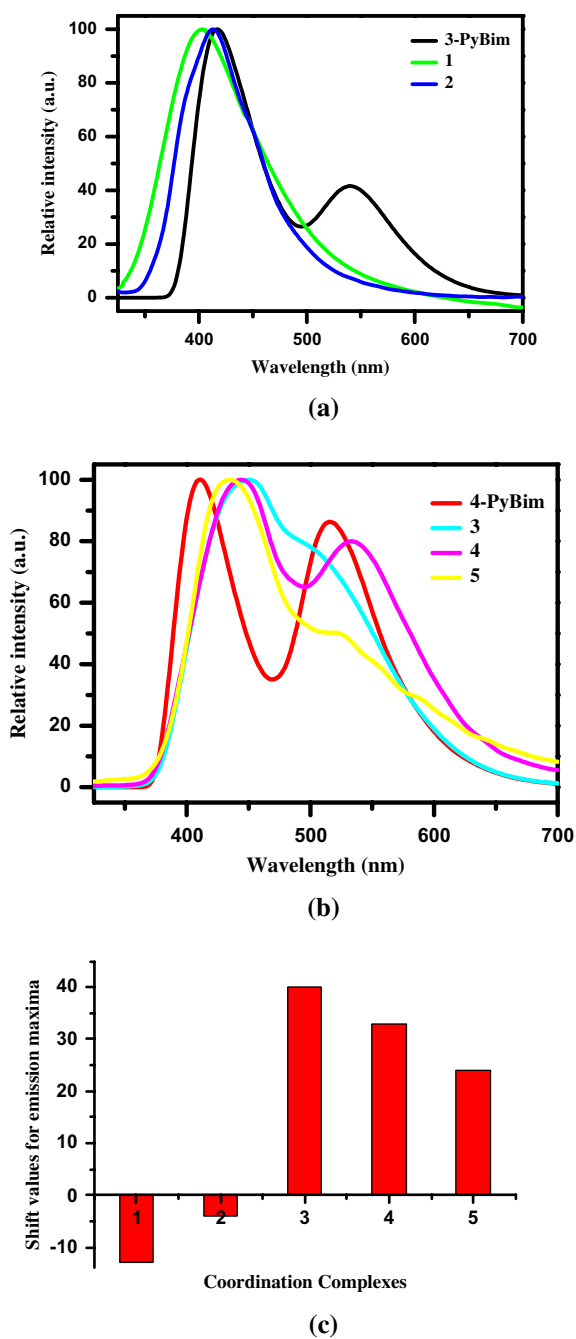


**Figure 6.** Fluorescence emission spectra of 3-PyBim, 4-PyBim and its complexes 1 and 2 (a), and 3–5 (b) in the solid state at room temperature. (c) Comparison of emission maxima for 1–5.

than those of the free ligands, which could be a consequence of coordination of the ligand, increasing the rigidity of the ligand, thereby reducing the loss of energy through a radiationless pathway [30].

**Table 5.** Photoluminescent properties for **3-PyBim**, **4-PyBim** and **1–5**.

Compounds	Emission maxima	$\Delta^a$
<b>3-PyBim</b>	417	
<b>1</b>	404	–13
<b>2</b>	413	–4
<b>4-PyBim</b>	411	
<b>3</b>	451	+40
<b>4</b>	444	+33
<b>5</b>	435	+24

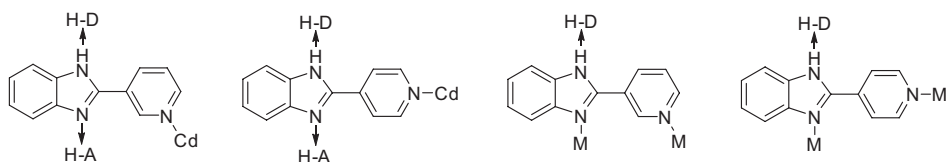
<sup>a</sup> $\Delta$ : The shift values for **3-PyBim**, **4-PyBim** and **1–5**. The symbols ‘–’ and ‘+’ are represented as blue-shifted and red-shifted, respectively.

Photoluminescent complexes with **3/4-PyBim** have been investigated. Complexes such as  $[\text{Ag}_2(4\text{-PyBim})_2(\text{H}_2\text{O})_2]\text{SO}_4 \cdot \text{H}_2\text{O}$  [21b],  $[\text{Co}(3\text{-PyBim})_2(\text{H}_2\text{O})_2\text{Mo}_6\text{O}_{20}]$  [21c],  $[\text{Cu}_2(\text{CN})_2(3\text{-PyBim})_n]$  [21e],  $[\text{Ag}(4\text{-PyBim})(\text{H}_2\text{O})(\text{NO}_3)]_n$  [21f] and  $[\text{Cu}_2(\text{SCN})_2(4\text{-PyBim})_n]$  [21g] display interesting photoluminescent properties, with emission located at 540, 446, 440, 394, and 569 nm, respectively, similar to those observed in the present work. Comparison with the photoluminescent behaviors of ligands **3-PyBim** and **4-PyBim**, those of complexes are blue-shifted and red-shifted in the present work.

The blue-shifted magnitude of **1** is much smaller than that of **2**. The red-shifted extent gradually decreases from **3** to **5**. Consequently, we propose that when the electronegativity of the coordinated atoms from the coordinated anions was increased, the blue/red-shift was raised. To further investigate whether there exists a relationship between the structures and the emission properties among these complexes, we examined the nature of the coordination environment of Cd(II). As illustrated in the description of crystal structures for **1–5**, there are significant differences from the coordinated anions,  $\text{SO}_4^{2-}$ ,  $\text{I}^-$ ,  $\text{Cl}^-$ ,  $\text{Br}^-$  and  $\text{I}^-$  for **2**, **1**, **3**, **4**, and **5**, respectively. In **2**, there only exist nitrogens and oxygens. However, in **1**, with coordinated N and O, there is iodide. The extent of blue-shift for **2** is much stronger than that of **1** (Figure 6(c)). The electronegativity of oxygen in **2** is much higher than that of iodide in **1**. We suggest that the electronegativity of the coordinated atoms accounts for the extent of blue-shift but also the shift is proportional to the electronegativity of the coordinated atoms. The interesting results encourage us to further investigate whether there exists a structure-property relationship among **3–5** and the specific structure-activity relationship was also found among these complexes. It is clear that there are different coordinated ions, chloride, bromide, and iodide. Electronegativity decreases from Cl to I. The red-shifted values of luminescent properties for **3–5** are 40, 33, and 24 nm, respectively (Table 5 and Figure 6(c)). The present observation further confirmed the fact that the shift of photoluminescence is proportional to the electronegativity of the coordinated atoms among these complexes. The observed blue- or red-shift of the emission maximum may be tentatively attributed to the following reasons: (i) after the ligands coordinated with metal ions, they may affect their lowest occupied molecular orbital (LUMO) and highest occupied molecular orbital (HOMO) energy levels; (ii) complexes may have charge-transfer transitions between Cd(II) centers and ligands [21f,g].

### 3.4. Difference of the coordination modes between **3-PyBim** and **4-PyBim**

The N from pyridinyl group in the **3/4-PyBim** binds monodentate to metal ions. The two nitrogens of benzimidazole groups play a role as donor and acceptor for hydrogen bonds, affecting the solid structures. To further investigate these coordination modes and hydrogen



**Scheme 2.** The coordination modes for **3-PyBim** and **4-PyBim**.

bonds of **3/4-PyBim** complexes, we summarize the structural features of reported complexes with **3/4-PyBim** ligands [21]. There exist three potential coordination sites in **3/4-PyBim** ligands (two nitrogens from benzimidazole and one nitrogen from pyridinyl ring). (i) In the present work, the **3/4-PyBim** ligands use N from pyridine to bind Cd(II) (Scheme 2), similar with the coordination mode of **3/4-PyBim** observed in  $[\text{Cu}(\mathbf{3-PyBim})_2(\text{H}_2\text{O})_2](\text{ClO}_4)_2$ ,  $[\text{Co}(\mathbf{3-PyBim})_2(\text{H}_2\text{O})_4](\text{NO}_3)_2 \cdot (\text{H}_2\text{O})_4$ ,  $[\text{Cu}(\mathbf{4-PyBim})_2(\text{Cl})_2](\text{H}_2\text{O})_2$ ,  $[\text{Zn}(\mathbf{4-PyBim})_2(\text{H}_2\text{O})_2(\text{NO}_3)_2]$ , and  $[\text{Cu}_2(\mathbf{3-PyBim})_2(\text{OAc})_4]$  [21a]. As a result, these complexes display a zero-dimensional motif. (ii) The ligands possess the 'end-on' binding with a hydrogen-bond donor (H-D) and acceptor (H-A), comparable to reported results [21a]. These features provide weak interaction sites for the construction of supramolecular architectures. In **1**, two adjacent units are connected by  $\text{O-H} \cdots \text{N}$  hydrogen bonds between free water molecules and nitrogens from benzimidazole rings, resulting in a 1-D chain along the *a* axis. Similarly, in **2**,  $\text{N-H} \cdots \text{O}$  hydrogen bonds are generated through nitrogens from benzimidazole and oxygens from sulfate, giving a 1-D chain. In **3–5**, a 2-D supramolecular layer is formed by  $\text{O-H} \cdots \text{N}$  hydrogen bonds between coordinated water and nitrogens from the benzimidazole groups of these 1-D supramolecular chains. Such results are also observed in other supramolecular assemblies [21a]. Finally, a 3-D supramolecule is constructed by  $\text{N-H} \cdots \text{X}$  ( $\text{X} = \text{Cl}, \text{Br}, \text{I}$ ) hydrogen interactions on the basis of a 2-D supramolecular layer. Apart from these hydrogen bond interactions, there exist two kinds of weak  $\pi \cdots \pi$  packing interactions between aromatic rings to construct a 2-D supramolecular layer. The coordination modes of **3/4-PyBim** ligands are observed in the present work and some reported complexes, which are listed in Scheme 2. We anticipate other interesting coordination modes of **3/4-PyBim** when more coordination complexes with these ligands are explored.

## 4. Conclusion

We have prepared a set of Cd(II) coordination complexes that exhibit extended three-dimensional structures supported by two *N*-heterocyclic ligands through self-assembly under hydrothermal conditions. The photoluminescent properties can be tuned through the electronegativity of the coordinated counterions, with their blue/red-shift of luminescence decreased upon decrease of the electronegativity of the coordinated atoms. Further development of metal complexes with interesting photoluminescent properties is underway in our laboratory.

## Acknowledgements

We thank Ms Min Liu, Ms Nan-Nan Sun, and Mr Dan Liu for helping with experiments. We also thank the reviewers for giving many constructive comments.

## Disclosure statement

No potential conflict of interest was reported by the authors.

## Funding

This work was supported by the National Natural Science Foundation of China [grant number 21276149], Shandong Distinguished Middle-aged Young Scientist Encouragement and Reward Foundation [grant number BS2011CL034], Program for Scientific Research Innovation Team in Colleges and Universities of Shandong Province, International Cooperation Project for the Excellent Youth Scholars by Department of Education of Shandong Province, the Project of Shandong Province Higher Educational Science and Technology Program [grant number J09LB03].

## References

- [1] (a) Q.R. Fang, D.Q. Yuan, J. Sculley, J.R. Li, Z.B. Han, H.C. Zhou. *Inorg. Chem.*, **49**, 11637 (2010); (b) J. Tian, L.V. Saraf, B. Schwenzer, S.M. Taylor, E.K. Brechin, J. Liu, S.J. Dalgarno, P.K. Thallapally. *J. Am. Chem. Soc.*, **134**, 9581 (2012); (c) T.R. Cook, Y.-R. Zheng, P.J. Stang. *Chem. Rev.*, **113**, 734 (2013).
- [2] (a) M.D. Allendorf, C.A. Bauer, R.K. Bhakta, R.J.T. Houk. *Chem. Soc. Rev.*, **38**, 1330 (2009); (b) B.A. Blight, R.M. Guillet Nicolas, F. Kleitz, R.Y. Wang, S. Wang. *Inorg. Chem.*, **52**, 1673 (2013); (c) W. Wang, J. Yang, R.M. Wang, L.L. Zhang, J.F. Yu, D.F. Sun. *Cryst. Growth Des.*, **15**, 2589 (2015); (d) L. Cheng, J. Wang, Q. Qi, X. Zhang, H. Yu, S. Gou, L. Fang. *Cryst. Eng. Comm.*, **16**, 10056 (2014); (e) Y. Cui, B. Chen, G. Qian. *Coord. Chem. Rev.*, **273**, 76 (2014); (f) J. Zheng, Y.-D. Yu, F.-F. Liu, B.-Y. Liu, G. Wei, X.-C. Huang. *Chem. Commun.*, **50**, 9000 (2014); (g) L.L. Han, Y.X. Wang, Z.M. Guo, C. Yin, T.P. Hu, X.P. Wang, D. Sun. *J. Coord. Chem.*, **68**, 1754 (2015).
- [3] P. Horcajada, R. Gref, T. Baati, P.K. Allan, G. Maurin, P. Couvreur, G. Férey, R.E. Morris, C. Serre. *Chem. Rev.*, **112**, 1232 (2012).
- [4] (a) W. Zhang, R.G. Xiong. *Chem. Rev.*, **112**, 1163 (2012); (b) Y.T. Wang, G.M. Tang, W.Z. Wan, Y. Wu, T.C. Tian, J.H. Wang, C. He, X.F. Long, J.J. Wang, S.W. Ng. *CrystEngComm*, **14**, 3802 (2012); (c) Y.T. Wang, G.M. Tang, C. He, S.C. Yan, Q.C. Hao, L. Chen, X.F. Long, T.D. Li, S.W. Ng. *CrystEngComm*, **13**, 6365 (2011); (d) J.L. Qi, S.L. Ni, Y.Q. Zheng, W. Xu. *Solid State Sci.*, **28**, 61 (2014).
- [5] (a) C. Wang, T. Zhang, W. Lin. *Chem. Rev.*, **112**, 1084 (2012); (b) Y.T. Wang, G.M. Tang, Y.Q. Wei, T.X. Qin, T.D. Li, J.B. Ling, X.F. Long. *Inorg. Chem. Commun.*, **12**, 1164 (2009); (c) L. Cheng, H.Y. Hu, L.M. Zhang, S.H. Gou. *Inorg. Chem. Commun.*, **15**, 202 (2012); (d) Y.T. Wang, H.H. Fan, H.Z. Wang, X.M. Chen. *Inorg. Chem.*, **44**, 4148 (2005); (e) Y.-T. Wang, G.-M. Tang, C. He, S.-C. Yan, Q.-C. Hao, L. Chen, X.-F. Long, T.-D. Li, S.W. Ng. *CrystEngComm*, **13**, 6365 (2011).
- [6] (a) J.-P. Zhang, Y.-B. Zhang, J.-B. Lin, X.-M. Chen. *Chem. Rev.*, **112**, 1001 (2012); (b) A. Bétard, R.A. Fischer. *Chem. Rev.*, **112**, 1055 (2012); (c) J.-R. Li, J. Sculley, H.-C. Zhou. *Chem. Rev.*, **112**, 869 (2012); (d) J. Liu, P.K. Thallapally, B.P. McGrail, D.R. Brown. *J. Liu. Chem. Soc. Rev.*, **41**, 2308 (2012); (e) L.J. Murray, M. Dinca, J.R. Long. *Chem. Soc. Rev.*, **38**, 1294 (2009); (f) Y.B. Zhang, H.L. Zhou, R.B. Lin, C. Zhang, J.B. Lin, J.P. Zhang, X.M. Chen. *Nat. Commun.*, **3**, 642 (2012); (g) E.D. Bloch, W.L. Queen, R. Krishna, J.M. Zadrozny, C.M. Brown, J.R. Long. *Science*, **335**, 1606 (2012); (h) D. Hexiang, S. Grunder, K.E. Cordova, C. Valente, H. Furukawa, M. Hmadeh, F. Gandara, A.C. Whalley, L. Zheng, S. Asahina, H. Kazumori, M. O'Keeffe, O. Terasaki, J.F. Stoddart, O.M. Yaghi. *Science*, **336**, 1018 (2012); (i) H.-H. Wang, L.-N. Jia, L. Hou, W.-J. Shi, Z. Zhu, Y.-Y. Wang. *Inorg. Chem.*, **54**, 1841 (2015).
- [7] (a) S.M. Cohen. *Chem. Rev.*, **112**, 970 (2012); (b) D. Bradshaw, A. Garai. *J. Huo. Chem. Soc. Rev.*, **41**, 2344 (2012); (c) Y. Zhang, S.N. Riduan. *Chem. Soc. Rev.*, **41**, 2083 (2012); (d) L. Ma, C. Abney, W. Lin. *Chem. Soc. Rev.*, **38**, 1248 (2009); (e) M. Yoon, R. Srirambalaji, K. Kim. *Chem. Rev.*, **112**, 1196 (2012); (f) J. Liu, L. Chen, H. Cui, J. Zhang, L. Zhang, C.Y. Su. *Chem. Soc. Rev.*, **43**, 6011 (2014); (g) X.P. Wang, Y.Q. Zhao, Z. Jaglicic, S.N. Wang, S.J. Lin, X.Y. Li, D. Sun. *Dalton Trans.*, **44**, 11013 (2015); (h) L. Liu, Z.-B. Han, S.-M. Wang, D.-Q. Yuan, S.W. Ng. *Inorg. Chem.*, **54**, 3719 (2015); (i) J. Nan, J. Liu, H. Zheng, Z. Zuo, L. Hou, H. Hu, Y. Wang, X. Luan. *Angew. Chem. Int. Ed.*, **54**, 2356 (2015); (j) J.-H. Wang, G.-M. Tang, Y.-T. Wang, Y.-Z. Cui, J.-J. Wang, S.W. Ng. *Dalton Trans.*, **44**, 17829 (2015).

- [8] (a) F. Shao, J. Li, J.-P. Tong, J. Zhang, M.-G. Chen, Z. Zheng, R.-B. Huang, L.-S. Zheng. *Chem. Comm.*, **49**, 10730 (2013); (b) D.-F. Weng, Z.-M. Wang, S. Gao. *Chem. Soc. Rev.*, **40**, 3157 (2011); (c) E. Coronado, G. Minguez Espallargas. *Chem. Soc. Rev.*, **42**, 1525 (2013); (d) M. Kurmoo. *Chem. Soc. Rev.*, **38**, 1353 (2009); (e) J. Tao, R.J. Wei, R.B. Huang, L.S. Zheng. *Chem. Soc. Rev.*, **41**, 703 (2012); (f) L. Cheng, W.X. Zhang, B.H. Ye, J.B. Lin, X.M. Chen. *Eur. J. Inorg. Chem.*, **2007**, 2668 (2007); (g) M.-H. Zeng, Z. Yin, Y.-X. Tan, W.-X. Zhang, Y.-P. He, M. Kurmoo. *J. Am. Chem. Soc.*, **136**, 4680 (2014); (h) C.-F. Wang, R.-F. Li, X.-Y. Chen, R.-J. Wei, L.-S. Zheng. *J. Tao. Angew. Chem. Int. Ed.*, **54**, 1574 (2015); (i) M.L. Tong, J. Wang, S. Hu. *J. Solid State Chem.*, **178**, 1518 (2005); (j) Y.T. Wang, G.M. Tang, Y.C. Zhang, W.Z. Wan, J.C. Yu, T.D. Li, Y.Z. Cui. *J. Coord. Chem.*, **63**, 1504 (2010).
- [9] (a) B.H. Ye, M.L. Tong, X.M. Chen. *Coord. Chem. Rev.*, **249**, 545 (2005); (b) Z.J. Lin, M.L. Tong. *Coord. Chem. Rev.*, **255**, 421 (2011); (c) J.Y. Zhang, C.Y. Su. *Coord. Chem. Rev.*, **257**, 1373 (2013); (d) D. Sun, Z.H. Yan, M.J. Liu, H.Y. Xie, S. Yuan, H.F. Lu, S.Y. Feng, D.F. Sun. *Cryst. Growth Des.*, **12**, 2902 (2012); (e) S. Hu, F.Y. Yu, P. Zhang, D.R. Lin. *Dalton Trans.*, **42**, 7731 (2013); (f) S. Hu, F.Y. Yu, P. Zhang, A.J. Zhou. *Eur. J. Inorg. Chem.*, **2012**, 3669 (2012); (g) J.H. Wang, G.M. Tang, Y.T. Wang, T.X. Qin, S.W. Ng. *CrystEngComm*, **16**, 2660 (2014); (h) J.-H. Wang, G.-M. Tang, T.-X. Qin, S.-C. Yan, Y.-T. Wang, Y.-Z. Cui, S. Weng Ng. *J. Solid State Chem.*, **219**, 55 (2014); (i) Y.T. Wang, G.M. Tang. *J. Coord. Chem.*, **60**, 2139 (2007).
- [10] (a) Y. He, B. Li, M. O’Keeffe, B. Chen. *Chem. Soc. Rev.*, **43**, 5618 (2014); (b) J.P. Zhang, Y.B. Zhang, J.B. Lin, X.M. Chen. *Chem. Rev.*, **112**, 1001 (2012); (c) Y.T. Wang, W.Z. Wan, G.M. Tang, Z.W. Qiang, T.D. Li. *J. Coord. Chem.*, **63**, 206 (2010); (d) Y.-G. Sun, J. Li, J. You, Y. Guo, G. Xiong, B.-Y. Ren, L.-X. You, F. Ding, S.-J. Wang, F. Verpoort, I. Dragutan, V. Dragutan. *J. Coord. Chem.*, **68**, 1199 (2015).
- [11] (a) J. Ni, K.J. Wei, Y.Z. Liu, X.C. Huang, D. Li. *Cryst. Growth Des.*, **10**, 3964 (2010); (b) U.P. Singh, S. Kashyap, H.J. Singh, R.J. Butcher. *CrystEngComm*, **13**, 4110 (2011).
- [12] (a) B. Zheng, H. Dong, J.F. Bai, Y.Z. Li, S.H. Li, M. Scheer. *J. Am. Chem. Soc.*, **130**, 7778 (2008); (b) P. Kanoo, K.L. Gurunatha, T.K. Maji. *Cryst. Growth Des.*, **9**, 4147 (2009); (c) X.F. Wang, Y.B. Zhang, W. Xue, X.L. Qi, X.M. Chen. *CrystEngComm*, **12**, 3834 (2010); (d) Q.H. Chen, F.L. Jiang, L. Chen, M. Yang, M.C. Hong. *Chem. Eur. J.*, **18**, 9117 (2012); (e) Y.Y. Yin, X.Y. Chen, X.C. Cao, W. Shi, P. Cheng. *Chem. Commun.*, **48**, 705 (2012).
- [13] (a) D. Liu, Z.G. Ren, H.X. Li, Y. Chen, J. Wang, Y. Zhang, J.P. Lang. *CrystEngComm*, **12**, 1912 (2010); (b) L.S. Long. *CrystEngComm*, **12**, 1354 (2010); (c) H.X. Yang, S.Y. Gao, J. Lu, B. Xu, J.X. Lin, R. Cao. *Inorg. Chem.*, **49**, 736 (2010); (d) F. Pannetier, G. Ohanessian, G. Frison. *Dalton Trans.*, **40**, 2696 (2011); (e) D. Sun, Z.H. Wei, C.F. Yang, D.F. Wang, N. Zhang, R.B. Huang, L.S. Zheng. *CrystEngComm*, **13**, 1591 (2011); (f) A.B. Lago, R. Carballo, S. Rodriguez-Hermida, E.M. Vazquez-Lopez. *CrystEngComm*, **15**, 1563 (2013).
- [14] (a) C.P. Li, M. Du. *Chem. Commun.*, **47**, 5958 (2011); (b) J. Xiao, B.Y. Liu, G. Wei, X.C. Huang. *Inorg. Chem.*, **50**, 11032 (2011); (c) M. Felloni, A.J. Blake, P. Hubberstey, C. Wilson, M. Schröder. *Cryst. Growth Des.*, **9**, 4685 (2009).
- [15] J. Guo, J.F. Ma, B. Liu, W.Q. Kan. *J. Yang. Cryst. Growth Des.*, **11**, 3609 (2011).
- [16] (a) J. Xiao, Y. Wu, M. Li, B.Y. Liu, X.C. Huang, D. Li. *Chem-Eur. J.*, **19**, 1891 (2013); (b) Y.Q. Wei, Y.F. Yu, R.J. Sa, Q.H. Li, K.C. Wu. *CrystEngComm*, **11**, 1054 (2009).
- [17] C.X. Ding, X. Rui, C. Wang, Y.S. Xie. *CrystEngComm*, **16**, 1010 (2014).
- [18] E.C. Yang, Y.N. Chan, H. Liu, Z.C. Wang, X.J. Zhao. *Cryst. Growth Des.*, **9**, 4933 (2009).
- [19] (a) V.K. Au, W.H. Lam, W.T. Wong, V.W. Yam. *Inorg. Chem.*, **51**, 7537 (2012); (b) Y. Cui, Y. Yue, G. Qian, B. Chen. *Chem. Rev.*, **112**, 1126 (2012).
- [20] (a) H.Y. Liu, J.F. Ma, Y.Y. Liu, J. Yang. *CrystEngComm*, **15**, 2699 (2013); (b) C.Y. Su, X.P. Yang, S. Liao, T.C.W. Mak, B.S. Kang. *Inorg. Chem. Commun.*, **2**, 383 (1999).
- [21] (a) X.P. Li, M. Pan, S.R. Zheng, Y.R. Liu, Q.T. He, B.S. Kang, C.Y. Su. *Cryst. Growth Des.*, **7**, 2481 (2007); (b) C.K. Xia, C.Z. Lu, Q.Z. Zhang, X. He, J.J. Zhang, D.M. Wu. *Cryst. Growth Des.*, **5**, 1569 (2005); (c) L.J. Chen, X. He, C.K. Xia, Q.Z. Zhang, J.T. Chen, W.B. Yang, C.Z. Lu. *Cryst. Growth Des.*, **6**, 2076 (2006); M.H. Zeng, L.J. Zhang, H. Liang. *J. Coord. Chem.*, **62**, 886 (2009); (e) H. Wang, M.-X. Li, M. Shao, X. He. *Polyhedron*, **26**, 5171 (2007); (f) N. Kundu, A. Audhya, S.M.T. Abtab, S. Ghosh, E.R.T. Tiekink, M. Chaudhury. *Cryst. Growth Des.*, **10**, 1269 (2010); (g) M.X. Li, H. Wang, S.W. Liang, M. Shao, X. He, Z.X. Wang, S.R. Zhu. *Cryst. Growth Des.*, **9**, 4626 (2009); (h) Y.-X. Zhou, X. Li, H.-Y. Zhang, C.-L. Fan, H.-Y. Zhang, B.-L. Wu. *J. Coord. Chem.*, **64**, 4066 (2011); (i) H.Y. Liu, L. Bo, J. Yang, Y.Y. Liu, J.F. Ma, H.

- Wu. *Dalton Trans.*, **40**, 9782 (2011); (j) C.J. Wang, K.F. Yue, Z.X. Tu, L.L. Xu, Y.L. Liu, Y.Y. Wang. *Cryst. Growth Des.*, **11**, 2897 (2011).
- [22] S.-Y. Lin, Y. Isome, E. Stewart, J.-F. Liu, D. Yohannes, L. Yu. *Tetrahedron Lett.*, **47**, 2883 (2006).
- [23] (a) M. Dey, K. Deb, S.S. Dhar. *Chin. Chem. Lett.*, **22**, 296 (2011); (b) H.N. Kim, H.K. Lee, S.W. Lee. *Bull. Korean Chem. Soc.*, **26**, 892 (2005).
- [24] G.M. Sheldrick, *SADABS*, University of Göttingen, Göttingen (1996 and 2003).
- [25] A.X.S. Bruker. *SAINT Software Reference Manual*, Bruker Company, Madison, WI (1998).
- [26] (a) G.M. Sheldrick, *SHELXTL NT Version 5.1. Program for Solution and Refinement of Crystal Structures*, University of Göttingen, Germany (1997); (b) G.M. Sheldrick. *Acta Crystallogr., Sect. A*, **64**, 112 (2008).
- [27] A.L. Spek. *J. Appl. Cryst.*, **36**, 7 (2003).
- [28] X.M. Chen, J.W. Cai. *Single-Crystal Structural Analysis Principles and Practices.*, Science Press, Beijing (2003).
- [29] (a) L.H. Cao, Y.L. Wei, Y. Yang, H. Xu, S.Q. Zang, H.W. Hou, T.C.W. Mak. *Cryst. Growth Des.*, **14**, 1827 (2014); (b) V.W.W. Yam, K.K.W. Lo. *Chem. Soc. Rev.*, **28**, 323 (1999).
- [30] B.R. Masters. *Molecular Fluorescence: Principles and Applications*, 2nd Edn, Wiley-VCH, Weinheim (2012).